Synthesis and electrochemical properties of SnO$_2$-CuO nanocomposite powders

MA Ming-you(麻明友)[1], HE Ze-qiang(何则强)[1,2], XIAO Zhuo-bing(肖卓炳)[1],
HUANG Ke-long(黄可龙)[2], XIONG Li-zhi(熊利芝)[1], WU Xian-ming(吴显明)[1]

1.College of Chemistry and Chemical Engineering, Jishou University, Jishou 416000, China;
2.School of Chemistry and Chemical Engineering, Central South University, Changsha 410083, China
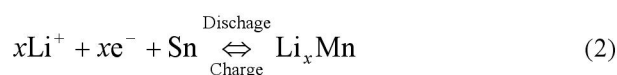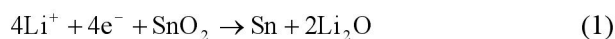
Abstract: SnO$_2$-CuO nanocomposite powders were prepared by chemical coprecipitation method using SnCl$_4$·5H$_2$O, NH$_3$·H$_2$O and Cu(NO$_3$)$_2$·3H$_2$O as raw materials. The powders were characterized by thermogravimertric(TG) analysis and differential thermal analysis(DTA), X-ray diffraction(XRD), and scanning electron microscope(SEM). The electrochemical properties of SnO$_2$-CuO and undoped SnO$_2$ powders as anode materials of lithium ion batteries were investigated comparatively by galvanostatic charge-discharge experiments and AC impedance. The results show that SnO$_2$-CuO nanocomposite powders with the average particle size of 87 nm can be obtained by this method. The structure of SnO$_2$ does not change with the introduction of CuO, but the average particle size of nano-SnO$_2$ decreases. SnO$_2$-CuO nanocomposite powders show a reversible capacity of 752 mA·h/g and better cycleability compared with nano-SnO$_2$. The capacity retention rates after 60 cycles of nano-SnO$_2$-CuO and SnO$_2$ are 93.6% and 92.0% at the charge-discharge rate of 0.1 C, respectively, which suggests that the introduction of CuO into SnO$_2$ can improve the cycleability of nano-SnO$_2$.

Key words: SnO$_2$; CuO; chemical coprecipitation method; lithium ion batteries; electrochemical properties

1 Introduction

Since YOSHIO et al[1] announced the commercialization of tin oxide as negative electrodes of lithium-ion batteries, the tin oxide anode has attracted much attention due to its high specific capacity, which is about twice that of graphite, and has been considered the best candidate for lithium-ion battery anode material[2−7]. When SnO$_2$ was used as the anode material of lithium-ion batteries, tin works as the virtual part, and its reversible capacity is based on the formation and decomposition of lithium tin alloys, LiSn, Li$_7$Sn$_3$, Li$_5$Sn$_2$, Li$_3$Sn$_5$, Li$_7$Sn$_2$ or Li$_{22}$Sn$_5$[8]. The oxygen in SnO$_2$ can combine with lithium to form Li$_2$O in the first cycle, which acts as the buffer for tin aggregation. Lithium intercalating in tin dioxide in the first cycle can be described by the following reactions[2,9,10]:

$$4Li^+ + 4e^- + SnO_2 \rightarrow Sn + 2Li_2O \qquad (1)$$

$$xLi^+ + xe^- + Sn \underset{Charge}{\overset{Discharge}{\Leftrightarrow}} Li_xMn \qquad (2)$$

Different synthetic techniques can make SnO$_2$ with different particle sizes and morphologies, which can further affect its electrochemical performance. In this works, SnO$_2$-CuO was synthesized by chemical coprecipitation method and its electrochemical properties were investigated in detail.

2 Experimental

2.1 Preparation of SnO$_2$-CuO

A certain amount of SnCl$_4$·5H$_2$O and Cu(NO$_3$)$_2$·3H$_2$O at a mass ratio of w(CuO):w(SnO$_2$) =1:10 was dissolved in de-ionized water to get a mixed aqueous solution. Then NH$_3$·H$_2$O was added into the solution dropwise under strong stirring to keep the pH value of the solution in the range of 8−9. When the reaction completed, an azury precipitation was formed. After aged at room temperature for 2 h, the precipitation was washed with water and ethanol until no Cl$^-$ can be detected by AgNO$_3$

in the washing liquid. After the precipitation was dried at 105 ℃ for 4 h, it was calcined at 600 ℃ for 3 h in air to obtain the product of SnO_2-CuO.

2.2 Material characterization

The thermal behavior of the precursor was investigated by thermogravimetric analysis(TGA) and differential thermal analysis(DTA) on a TGA-SDTA851^e thermal analysis system(Mettler Toledo Corp) from 25℃ to 800 ℃ in Ar atmosphere at a heating rate of 10 ℃/min. The phase of the samples was characterized by X-ray diffraction(XRD, Rigaku D/MAX-gA) with a mono-chromatic Cu K_α radiation (0.1540 5 nm). The surface morphology, composition of elements of the samples were analyzed by means of scanning electron microscope (SEM, JEOL JSM 5600LV). The grain size was calculated using the Scherrer formula of $D=0.89\lambda/\beta\sin\theta$, in which D is the crystalline size, λ is the wavelength of X-ray, and θ is the diffraction peak angle.

2.3 Electrode preparation and electrochemical characterization

The SnO_2-CuO was made into slurry with 80% SnO_2 powder, 10% acetylene black, and 10% polyvinylidene difluoride(PVDF) in N-methyl pyrolidinone(NMP). The mixture was then coated on copper foils followed by a drying in vacuum at 120 ℃ for 10 h to obtain the SnO_2-CuO electrode.

The electrochemical tests were conducted using a conventional coin-type(2025) cell, employing SnO_2-CuO as positive electrode, a polypropylene microporous separator, utilizing 1.0 mol/L $LiPF_6$ in ethylene carbonate/dimethyl carbonate (EC/DMC) (with an EC to DMC volume ratio of 1:1) as the electrolyte and lithium foil as negative electrode. The assembly was carried out in an Ar-filled glove box. The discharge-charge tests were done with a PCBT-110-8D battery tester under a constant current rate of 0.1C and a constant temperature of (25±0.01) ℃ in the voltage range of 0−1.0 V. The AC impedance measurement was carried out on CHI660B electrochemical station. Here, the discharge process means the process of Li^+ insertion into SnO_2-CuO electrode and the charge process means the process of Li^+ de-insertion out of SnO_2-CuO electrode.

3 Results and discussion

Fig.1 shows the TG-DTA curves of the precursor dried at 105 ℃. From DTA curve, a large endothermic peak appears at 123 ℃. The endothermic peak corresponds to a clear mass loss on the TG curve, which is caused by the evaporation of physically absorbed water on the surface of the precursor. Due to the decomposition of little NH_4Cl impurity in the precursor,

an unconspicuous endothermic peak appears at 234 ℃ and a tardigrade mass loss can be found on the TG curve. A great exothermic peak near 275 ℃ on DTA curve and obvious mass loss on TG curve are found, which may correspond to the decomposition of precursor to form SnO_2, CuO and $CuSnO_3$. Because $CuSnO_3$ is unstable and easy to decompose and form stable SnO_2-CuO, a small exothermic peak at 450 ℃ is seen in the DTA curve [11]. From the analysis of TG-DTA curves, it can be concluded that the crystallization of SnO_2-CuO takes place at 250−500 ℃.
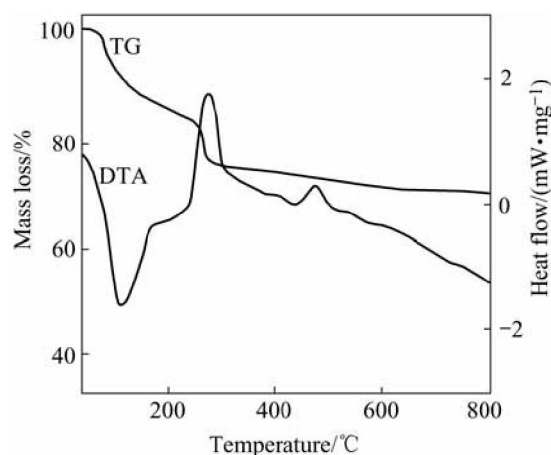

Fig.1 TG-DTA curves of precursor

The XRD patterns of SnO_2-CuO and undoped SnO_2 calcined at 500 ℃ for 3 h are presented in Fig.2. In the scan range from 10° to 90°, both the samples show the four major peaks (100), (101), (200) and (211), which correspond well with that of cassiterite phase (JCPDS file 41-1445). No diffraction peaks of CuO can be seen in Fig.2, which indicates that CuO has entered the crystal lattice and SnO_2-CuO solid solution is formed[12]. However, the peak half width of SnO_2-CuO is wider than that of SnO_2. According to Scherrer formula, we can calculate the crystal grain size of SnO_2-CuO to be 87 nm,
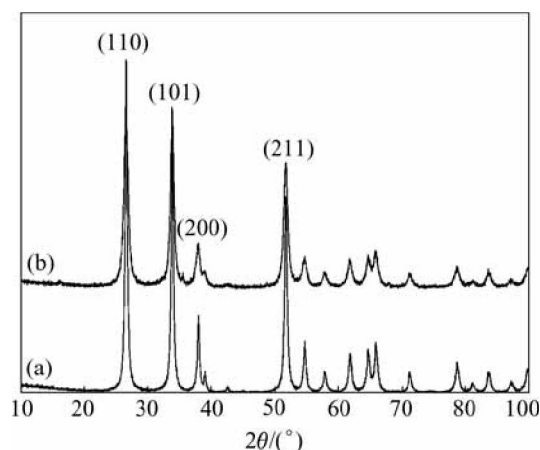

Fig.2 XRD patterns of nano SnO_2(a) and nano CuO-SnO_2 powders(b) calcined at 500 ℃ for 3 h

which is smaller than that of SnO_2, 92 nm. This shows the grain size of SnO_2 decreases with the doping of CuO, suggesting that the growth of the crystal of SnO_2 is depressed by the doping of CuO[13].

Fig.3 shows the morphologies of SnO_2-CuO and undoped SnO_2 calcined at 500 ℃ for 3 h. From Fig.3 we can see there is no essential difference between SnO_2-CuO and undoped SnO_2 and the average particle size is 80−90 nm. However, the particle size of SnO_2-CuO seems to be smaller than that of the undoped SnO_2, which agrees with the result of XRD analyses.
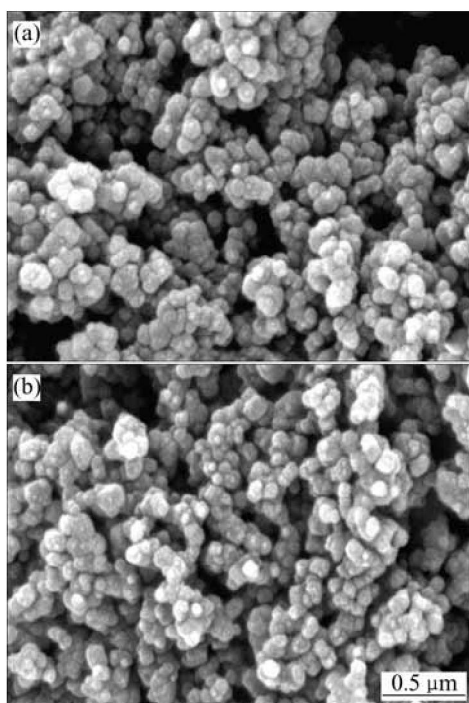

Fig.3 SEM images of nano SnO_2(a) and nano SnO_2-CuO(b) powders calcined at 500 ℃ for 3 h

Fig.4 shows the EDS results of nano SnO_2-CuO calcined at 500 ℃ for 3 h. As can be seen in the figure, except for Sn and Cu, no other metal element can be
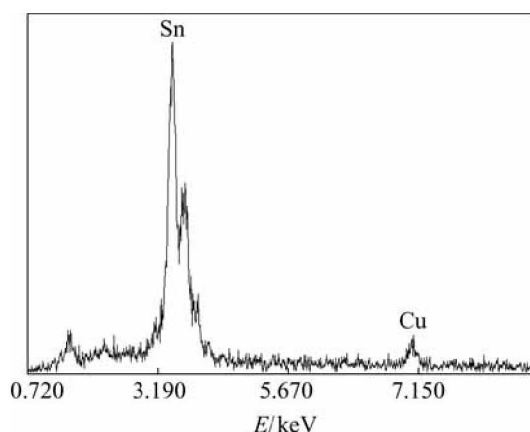

Fig.4 EDS results of nano SnO_2-CuO powders calcined at 500 ℃ for 1 h

detected, which indicates that the Cu element is doped into SnO_2. According to the EDS results, it can be calculated that the mass ratio of CuO to SnO_2 is 1:10.1, which agrees well with the mass ratio of 1:10.0, suggesting that the obtained sample is CuO-doped SnO_2.

The first discharge-charge curves of nano SnO_2 and nano SnO_2-CuO powders calcined at 500℃ for 3 h are shown in Fig.5. The first discharge-charge curves of nano SnO_2 and nano SnO_2-CuO are similar to each other, indicating that nano SnO_2-CuO has a similar mechanism of Li storage as nano SnO_2[2, 4]. The plateau between 1.0 V and 1.5 V in the discharging curves disappears in the latter cycle, corresponding well to the irreversible formation of Li_2O and solid-electrolyte interface(SEI) in the first discharging process[14]. They can give a total theoretical irreversible capacity of about 933 and 899 mA·h/g for nano SnO_2 and nano SnO_2-CuO, respectively. The plateau at 0.5−0.7 V in the discharge-charge curves is due to the reversible alloying process of lithium and tin, and it is the source of reversible capacity, which is about 760 and 752 mA·h/g for nano SnO_2 and nano SnO_2-CuO respectively.
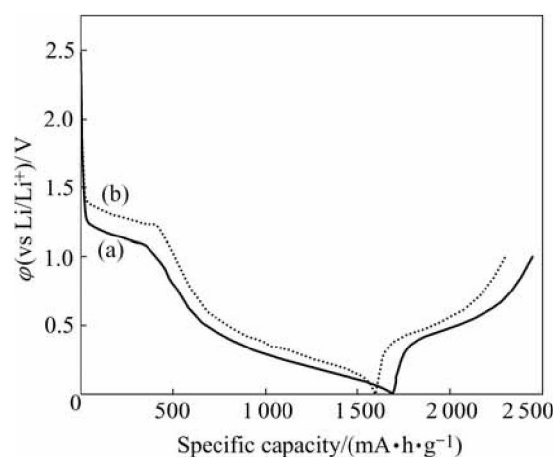

Fig.5 First discharge-charge curves of nano SnO_2(a) and SnO_2-CuO(b) (0.1C)

Fig.6 shows the variation of reversible capacity as a function of cycle number. For nano SnO_2, after 60 cycles the reversible capacity remains 92.0% that of the first cycle, the average capacity fade rate is 0.13% per cycle; while for nano SnO_2-CuO, the values are 93.6% and 0.11%, respectively. Compared with nano SnO_2, nano SnO_2-CuO anode has a smaller reversible capacity and better cycleability, which may result from the decreased mass of active material and particle size due to the doping of CuO.

Fig.7 shows the AC impedance diagram of nano SnO_2-CuO anode. Two semicircles and an inclined line can be seen in the figure. The high frequency arc is attributed to the charge-transfer reaction at the interface of electrolyte and electrode. The medium frequency arc

implies the formation of a new phase during the discharge and charge process, which may be caused by the formation of solid electrolyte interface(SEI) film on the surface of nano SnO_2-CuO[15]. The inclined line corresponds to Warburg impedance related to the diffusion of lithium ion in nano SnO_2-CuO anode [16].
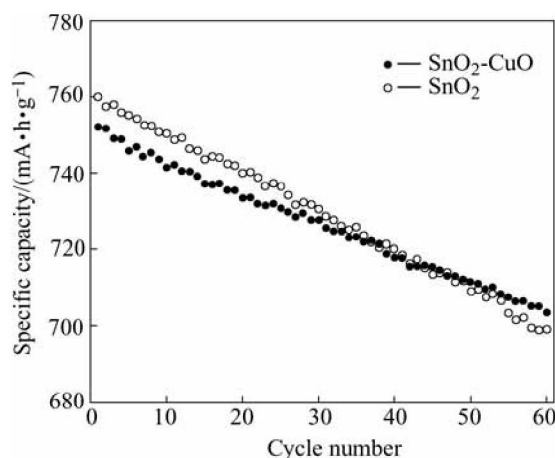

Fig.6 Cycleability of nano SnO_2-CuO and nano SnO_2 calcined at 500 ℃ for 3 h (0.1C)

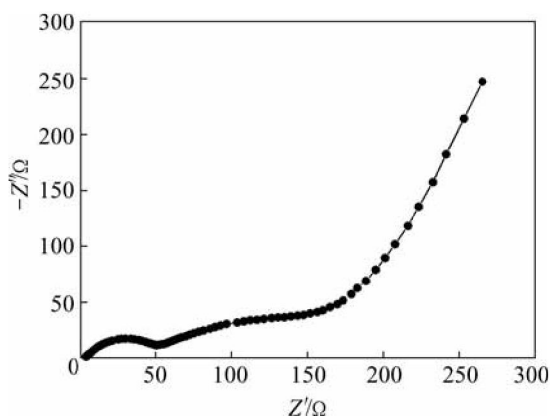**Fig.7** AC impedance diagram of nano SnO_2-CuO calcined at 600 ℃ for 3 h

4 Conclusions

Nano SnO_2-CuO were prepared by chemical co-precipitation method using $SnCl_4 \cdot 5H_2O$, $NH_3 \cdot H_2O$ and $Cu(NO_3)_2 \cdot 3H_2O$ as raw materials. The average particle size of synthesized SnO_2-CuO is 87 nm. The structure of SnO_2 does not change with the introduction of CuO, but the average particle size of nano-SnO_2 decreases. The nano SnO_2-CuO shows a reversible capacity of 752 mA·h/g and better cycleability compared with the undoped nano-SnO_2. The capacity retention rate after 60 cycles of nano SnO_2-CuO and SnO_2 is 93.6% and 92.0% at the charge-discharge rate of 0.1 C, respectively, which

suggests that the introduction of CuO in SnO_2 can improve the cycleability of nano-SnO_2.

References

[1]   YOSHIO I, TADAHIKO K. Tin-based amorphous oxide: a high-capacity lithium-ion storage material [J]. Science, 1997, 27(6): 1395−1397.

[2]   COURTNEY I A, DAHN J R. Electrochemical and in situ X-ray diffraction studies of the reaction of lithium with tin oxide composites [J]. J Electrochem Soc, 1997, 144(6): 2045−2052.

[3]   LIU W F, HUANG X J, WANG Z X, LI H, CHEN L Q. Studies of stannic oxide as an anode material for lithium-ion batteries [J]. J Electrochem Soc, 1998, 145(1): 59−62.

[4]   COURTNEY I A, DAHN J R. Key factors controlling the reversibility of the reaction of lithium with SnO_2 and Sn_2BPO_6 glass [J]. J Electrochem Soc, 1997, 144(9): 2943−2948.

[5]   HE Ze-qiang, LI Xin-hai, WU Xian-ming, HOU Zhao-hui, LIU En-hui, DENG Ling-feng, HU Chuan-yue, TIAN Hui-peng. Preparation and electrochemical properties of nanosized tin dioxide electrode material by sol-gel process [J]. Trans Nonferrous Met Soc China, 2003, 13(4): 998−1002.

[6]   HE Ze-qiang, LI Xin-hai, XIONG Li-zhi, LIU En-hui, HOU Zhao-hui. Preparation and electrochemical properties of tin-based composite oxide by high-energy ball-milling method [J]. Chinese Journal of Inorganic Chemistry, 2004, 20(1): 102−106.(in Chinese)

[7]   HE Ze-qiang, LI Xin-hai, XIONG Li-zhi, WU Xian-ming, XIAO Zhuo-bing, MA Ming-you. Wet chemical synthesis of tin oxide-based material for lithium ion battery anodes [J]. Materials Research Bulletin, 2005, 40(5): 861−868.

[8]   ANANI A, CROUCH-BAKER S, HUGGINS R A. Kinetic and thermodynamic parameters of several binary lithium alloy negative electrodes materials at ambient temperature[J]. J Electrochem Soc, 1987, 134(12): 3098−3102.

[9]   RETOUX R, BROUSSE T, SCHLEICH D M. High-resolution electron microscopy investigation of capacity fade in SnO_2 electrodes for lithium-ion batteries [J]. J Electrochem Soc, 1999, 146(7): 2472−2476.

[10]   BROUSSE T, RETOUX R, HERTERICH U, SCHLEICH M. Thin-film crystalline SnO_2-lithium electrodes [J]. J Electrochem Soc, 1998, 145(1): 1−4.

[11]   HONG Wei-liang, DIAO Li-hui, LIU Jian-hong, ZHAO Feng-qi, TIAO De-yu, WANG Fang. Preparation of SnO_2-CuO nanoparticles and their catalytic activity in thermal decomposition of cyclotrimethylene trinitramine [J]. Chinese Journal of Applied Chemistry, 2004, 21(8): 775−778.(in Chinese)

[12]   LIU Mei, ZHANG Xiao-fen, LIU Kai, LI Hai-bo. Preparation of CuO-SnO_2 nano-sized powders [J]. Songliao Journal(Natural Science Edition), 2002, 11(1): 32−34.(in Chinese)

[13]   FANG Guo-jia, LIU Zu-li, HU Yi-fan, YAO Kai-lun. Preparation and characterization of CuO-SnO_2 nanocrystalline powders by the sol-gel method [J]. Journal of Inorganic Materials, 1996, 11(3): 537−541. (in Chinese)

[14]   WACHTLER M, BESENHARD J O, WINTER M. Tin and tin-based intermetallics as new anode materials for lithium-ion cells [J]. J Power Sources, 2001, 94(2): 189−193.

[15]   MACDONALD J R. Impedance Spectroscopy [M]. New York: John Wiley & Sons, 1987. 69.

[16]   AURBACH D, EIN-ELI Y, CHUSID O, CARMELI Y, BABAI M, YAMIN H. The correlation between the surface chemistry and the performance of Li-carbon intercalation anodes for rechargeable "Rocking Chair" type batteries [J]. J Electrochem Soc, 1994, 141(3): 603−610.

(Edited by YUAN Sai-qian)